Article

pubs.acs.org/Biomac

Investigating the Mechanisms of Amylolysis of Starch Granules by Solution-State NMR

Andrew J. Baldwin,*[,†,‡] Danielle L. Egan,[§] Fredrick J. Warren,[§] Paul D. Barker,[†] Christopher M. Dobson,[†] Peter J. Butterworth,*[,§] and Peter R. Ellis*[,§]

[†]Department of Chemistry, University of Cambridge, Lensfield Road, Cambridge, CB2 1EW, United Kingdom

[§]Biopolymers Group, Diabetes and Nutritional Sciences Division, King's College London, Franklin-Wilkins Building, 150 Stamford Street, London, SE1 9NH, United Kingdom

Supporting Information

ABSTRACT: Starch is a prominent component of the human diet and is hydrolyzed by α-amylase post-ingestion. Probing the mechanism of this process has proven challenging, due to the intrinsic heterogeneity of individual starch granules. By means of solution-state NMR, we demonstrate that flexible polysaccharide chains protruding from the solvent-exposed surfaces of waxy rice starch granules are highly mobile and that during hydrothermal treatment, when the granules swell, the number of flexible residues on the exposed surfaces increases by a factor of 15. Moreover, we show that these flexible chains are the primary substrates for α-amylase, being cleaved in the initial stages of hydrolysis. These findings allow us to conclude that the quantity of flexible α-glucan chains protruding from the granule surface will greatly influence the rate of energy acquisition from digestion of starch.

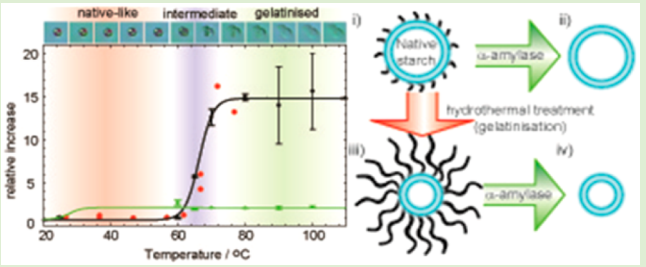

INTRODUCTION

Starch granules are energy storage components formed within plant cells. The granules are insoluble in water yet still accessible to the plant's metabolic enzymes.[1] With the development of cooking methods by hominids, the emergence of the ability to hydrolyze most of any starch ingested from plants with the enzyme α-amylase and therefore benefit from the energy source, represents a major development in the course of human evolution.[2−5] The energetic advantages arising from digestion of starch are believed to be of great importance in supporting the evolution of increased brain size.[6] In contrast to animal feedstuff, nearly all ingested starch in human diets will have been subjected to hydrothermal treatment during domestic and commercial food processing. Such starch is normally a main source of exogenous glucose produced during digestion that subsequently appears at high concentrations in the blood circulation.[7]

Cooked starch is digested rapidly in the gastrointestinal tract causing peaks in glycemia and insulinemia within 1 h after ingestion, but the rates of digestion of different starch sources can differ noticeably.[8] Controlling the variations in postprandial glycemia and insulinemia is of great importance in the prevention and treatment of diabetes mellitus and cardiovascular disease and also has implications for obesity management.[9−14] Thus, it is important that the relatively early stages of interaction between starch and α-amylase, the enzyme that catalyzes the first stage in the intestinal digestion of starch, are fully understood so that better predictions can be made of intestinal digestibility rates of particular starch sources and of the subsequent glycemia and insulinemia.

Solution-state NMR is uniquely powerful for observing dynamic segments of macromolecular assemblies.[15−17] If a segment within a complex assembly has a high degree of conformational flexibility, the effective local tumbling rate can be substantially greater than that expected for a rigid system of the same size, a phenomenon that results in significantly narrower NMR signals from such regions. A particularly interesting situation arises when flexible segments of a macromolecular assembly give rise to sharp NMR signals, whereas signals from the rigid core are too broad to be detected. This situation has been observed in studies of large functional biomolecular complexes, including ribosomes and protein aggregates, such as amyloid fibrils.[18−24] NMR experiments that are particularly useful for characterizing the resonances from flexible regions of significantly larger structures use pulsed field gradients (PFGs) to measure diffusion coefficients.[25] Such experiments measure physical displacement of nuclear spins during a delay denoted by Δ. Translational diffusion occurring in solution leads to the displacement of nuclear spins and so NMR diffusion experiments have traditionally been interpreted in terms of this phenomenon.[26] In recent years, however, it has been shown that for biomolecular assemblies with at least one dimension exceeding

Received: February 9, 2015
Revised: March 26, 2015
Published: March 27, 2015

DOI: 10.1021/acs.biomac.5b00190
Biomacromolecules 2015, 16, 1614−1621

about 500 nm, rotational, as well as translational motion, can influence NMR diffusion measurements.[27] These rotational effects are manifest as a variation in the apparent diffusion coefficients obtained from flexible segments at different values of Δ.[27,28] From such behavior, the size of the underlying structure can be deduced.[28] These methods are well suited for interrogating the structure of starch granules.

From a structural perspective, starch granules, which are supramolecular assemblies, are composed of the glucose polymers amylose and amylopectin, both containing primarily α-1,4 linkages. Amylopectin, normally ∼70−85% of the total polysaccharide, is highly branched via additional α-1,6 linkages, whereas the minority component amylose, ∼15−30%, possesses significantly fewer branch points and is essentially linear.[1,29,30] The granules possess regions of high (crystalline) and low (amorphous) local order, arranged with radial symmetry[30−32] that gives rise to a Maltese cross birefringence pattern when granules are viewed using cross-polarized light. Starch is hydrolyzed by α-amylases in the mouth and small intestine to low molecular-weight carbohydrates, such as maltose and maltotriose. There is considerable variation, however, in both the rate and the extent of starch digestion and the ensuing rise in blood glucose and insulin concentrations[8−11] that partly reflect differences in the underlying structures of the ingested starch granules.[30−32] We have shown recently that both the rate and the strength of binding of α-amylase to starch granules depends on the surface properties of the granule; binding to relatively smooth surfaces occurs more rapidly and with greater affinity than to surfaces with irregular contours.[33,34] It has been suggested that such findings provide strong evidence for the validity of the blocklet model of starch structure.[33] Also, a very recent report presents evidence that amylase binds to granule regions that are particularly susceptible to amylolysis.[35] Regions of high sensitivity to hydrolysis by α-amylase are crucial for amylolysis in nature,[1] but characterization of these regions has proven to be exceedingly challenging.

On hydrothermal treatment, the granules swell significantly when water is abundant and the Maltese cross birefringence pattern is lost in a process known as gelatinization.[30,36−41] This renders starch granules significantly more susceptible to digestion by α-amylase[1,42] and can be exploited industrially for products such as adhesives, alcoholic beverages, biofuels, and paper, and in the production of some organic chemicals.[1] In the present study, we demonstrate that flexible chains protruding from solvent-exposed surfaces of waxy rice starch granules (in which 94% of the starch polymer is amylopectin) can be observed using solution-state NMR techniques. Also, we establish that the number of disordered glucan chains increases as the granules swell after gelatinization and that these chains are removed in the early stages of hydrolysis by α-amylase. We show further that the number of flexible glucan chains on the granule surface is proportional to the exposed α-amylase reaction sites, leading to the conclusion that the flexible chains are the primary substrate for α-amylase. These NMR experiments provide direct experimental evidence that exposed surfaces of a starch granule possess flexible protruding chains[43] and that initial actions of α-amylase cause the removal of these chains leaving a central core. It follows that the flexibility of polysaccharide chains on the surface of starch granules is a primary determinant of the susceptibility of starch to amylolysis.

MATERIALS AND METHODS

Starch Samples. A waxy rice starch sample, Remyline-AX-DR (Cairn International Ltd., Chesham, Buckinghamshire, HP5 2JD, U.K.), was selected for its ease of dispersion in water for NMR measurements and for its homogeneity in shape and size when compared to starch from other sources. The nonstarch components of native granules were determined[44] and found to comprise (w/w): water, 12.4%; nonstarch polysaccharides, 1.3%; lipid, 0.2%; ash (total minerals), 0.3%; and protein, 0.09%. The total starch content of the samples was 85.7%. The relative amounts of amylopectin and amylose determined by a commercial assay kit (K-Amyl; Megazyme International Ireland, County Wicklow, Ireland) were found to be 94% and 6%, respectively. The native starch sample was examined by scanning electron microscopy (SEM) by mounting the sample on aluminum microscopy stubs using sticky tabs. The stubs were then sputter coated with gold before being examined and photographed using a high vacuum mode, high resolution electron microscope (FEI Quanta 200F SEM). Particle size analysis was performed using both Coulter counter and microscopy methods. The former method employed the use of a Beckman Multisizer 3 Coulter Counter,[34] and for the microscopy technique, an integrated system was used, comprising an optical microscope (Nikon model Eclipse E600), JVC color video camera, video digitizer, and computer with in-house image analysis software to measure particle size and shape.

Assay of α-Amylase Activity. Porcine pancreatic α-amylase (PPA) (type 1A, DFP-treated) was obtained from Sigma-Aldrich Chemical Co., Poole, Dorset, U.K. The manufacturers quote an activity of 1333 units/mg protein for the preparation. Its protein content was checked using the bicinchoninic acid method,[33] and the purity of the preparation and the relative molecular weight (56 kDa) were confirmed by SDS-PAGE. For assays, a stock solution of 32 μg of enzyme per ml was prepared in phosphate buffered saline (PBS; Oxoid Ltd., Basingstoke, Hampshire, U.K.) containing 1 mg/mL of bovine serum albumin. Starch solutions ranging from 1.25 to 10 mg/mL were produced by adding PBS to starch samples that had been pretreated as described below. Reaction mixtures containing 4 mL of each starch mixture were transferred to plastic 15 mL Falcon tubes and placed on a rotating table (33.3 rpm) to provide end-over-end mixing in an incubator at 37 °C for 15 min. Sufficient enzyme stock solution was added to the incubation mixtures to provide a final PPA concentration of 1.54 nM. Aliquots of 300 μL were removed at 0, 4, 8, and 12 min after the start of the incubation and added immediately to microfuge tubes containing 300 μL of ice cold 0.3 M Na_2CO_3 stop solution. The tubes were centrifuged at 16200*g* (Heraeus Pico 17, Thermo Scientific) for 5 min to sediment residual starch and then the total reducing sugar content of the supernatants was estimated by a Prussian Blue method.[33,45,46] After color development the absorbance at 690 nm was recorded on a Cecil CE 2041 spectrophotometer and converted to maltose equivalents by reference to a maltose standard curve. Initial reaction rates were calculated and computer fitted to the Michaelis−Menten equation (Enzfitter software, Biosoft, Great Shelford, Cambridgeshire, U.K.) to determine K_M^{exp} and V_{max} values.

NMR. Suspensions (10 mg/mL) of waxy rice starch samples (native granules) were prepared in PBS, swirled gently for 1 min and transferred into a 5 mm NMR tube. The samples were then allowed to stand for 30 min where two well separated phases resulted from sedimentation. Optical microscopy (Leitz Laborlux K) was used to verify that the material in the pellet consisted of aggregated starch granules, the size distribution of which did not vary over the time scale of the NMR experiments (up to 16 h); the material in the pellet phase of the NMR tube fell outside the portion of the tube detected during experiments and therefore did not contribute to the signal. For enzyme digests followed by NMR, the starch was initially subjected to hydrothermal treatment at a number of temperatures ranging from 25 to 100 °C; samples at 25 °C are represented by native granules, before amylolysis at 37 °C. For this processing, starch−water samples were placed in sealed tubes and immersed in a water bath set at the required temperature for 10 min during which time the contents of the tubes were mixed continuously. The tubes were then removed and allowed

DOI: 10.1021/acs.biomac.5b00190
Biomacromolecules 2015, 16, 1614−1621

to stand for 10 min at room temperature (20 °C) before examination by NMR. When the concentration of flexible chains was to be quantified, the heating process was conducted within the NMR spectrometer. Optical microscopy was used to determine that the abundance of starch granules in the aqueous phase was not obviously affected by heating up to 80 °C.

NMR data were acquired at 500 MHz on Bruker Avance instruments with a cryogenic TCI probe and ATM-TXI probe for use above 37 °C. A pulsed field gradient stimulated echo (PFGSE) sequence with a 3−9−19 watergate solvent suppression (Bruker pulse sequence *stbpgp 1s19*) was used for the diffusion experiments at 27 °C with δ = 5.4 ms.[28] Diffusion coefficients (D_{eff}) were obtained for diffusion delays, Δ, between 50 ms and 1 s, as described in the Results and Discussion. Sample viscosity was monitored by measuring the self-diffusion of water and was found not to vary substantially between the starch preparations. Processing and fitting of such data have been described in greater detail elsewhere.[28] Experimental uncertainties were estimated by comparing the variation of measured decay constants between individually recorded frequencies in the region of the peak of interest. In a PFGSE NMR diffusion experiment, the observed integrated signal S_i is attenuated due to translational diffusion from a reference intensity S_0 by a factor given by the Stejskal−Tanner relation[26] $S_i = S_0 \exp(-D_{eff}\alpha^2\beta G\dagger^2)$, where $\alpha = \gamma\delta G_{max}$, γ is the gyromagnetic ratio of the observed nucleus, δ is the duration of the applied gradient, G_{max} is the maximum strength of the applied gradients, $\beta = \Delta - \delta/3$, Δ is the diffusion delay, $G\dagger = G/G_{max}$, where G is the experimentally applied gradient. Thus, a plot of ln S_i/S_0 $(\alpha^2\beta)^{-1}$ versus $G\dagger^2$ has a gradient of $-D_{eff}$. For solutions of small molecules such as maltose or even of globular proteins, only translational diffusion, D_T, contributions will be significant, and so $D_{eff} = D_T$. D_T can be interpreted using hydrodynamic models such as the Einstein−Stokes relation for a continuum solvent.[47] $D_T = k_BT/6\pi\eta R_H$, where k_B is Boltzmann's constant, T is the thermodynamic temperature, and η is the sample viscosity. A more general expression for the decay of signal, including the effects of rotational diffusion,[27] shows that in the case of a sphere

$$D_{eff} = D_T + R_H^2/3\beta \quad (1)$$

Through studying the variation of D_{eff} with Δ and by using a model for D_T, the effective hydrodynamic radius of the underlying particle R_H can be determined.[27,28]

RESULTS AND DISCUSSION

Samples of waxy rice starch granules were examined by both optical microscopy and SEM (Figure 1a) revealing roughly spherical particles of diameter about 6 μm, that exhibit the Maltese cross pattern under crossed-polarized light (see below). The ^{1}H NMR spectrum of a starch sample was obtained (Figure 1b(i), blue), and compared to that acquired from a pure sample of maltose (Figure 1b(ii), red), an α-1,4 linked disaccharide and main product of amylolysis.

The spectra of starch and maltose were found to be very similar in the region of 3−6 ppm. The resonances from starch were significantly broader than those of maltose, by a factor of approximately 10, suggesting they originate from a chemical species that is much larger than maltose. When the maltose spectrum is broadened after convolution with a 16 Hz exponential function, it closely resembles the starch spectrum convoluted with a 2 Hz exponential function (Figure 1b(ii), inset). In maltose, two resonances are observed in the region 5−6 ppm (Figure 1b(ii), yellow and blue bands), corresponding to the C1 protons (SI, Figure S1). The absence of reducing ends in the starch spectrum indicates the presence of an extended maltose polymer joined through C1 linkages, which in the case of waxy rice is predominantly amylopectin. After amylase addition and incubation for 2 h, the signal intensity of

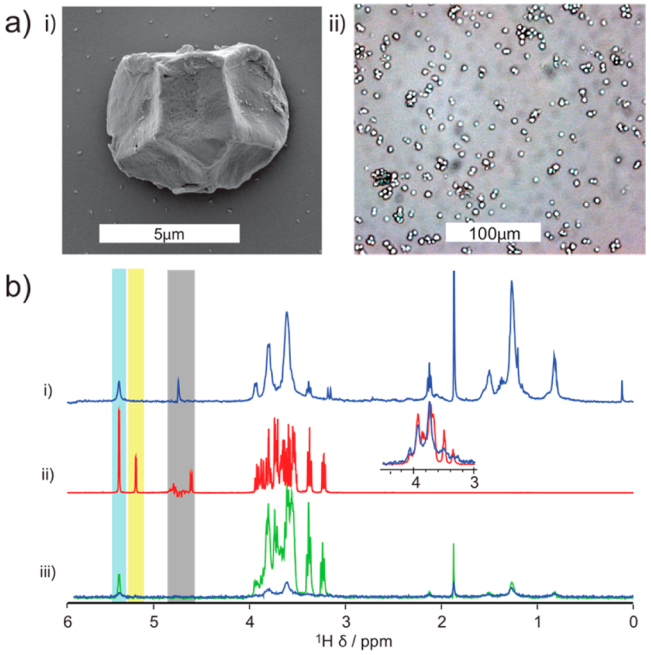

Figure 1. Microscopic and spectroscopic properties of starch granules. (a) Typical waxy rice starch granules as viewed using (i) Scanning Electron Microscopy (SEM) and (ii) optical microscopy. (b) The ^{1}H solution state NMR spectra of starch granules (i, blue), maltose (ii, red) and starch granules before and after digestion by α-amylase (iii, blue and green, respectively). The inset in ii shows superimposed convoluted spectra of starch (blue) and maltose (red).

the saccharide protons increased by a factor of 10 (Figure 1b(iii), green). The gray box in Figure 1b indicates incompletely suppressed resonances from H_2O.

To determine whether the observed NMR signals in the starch spectrum originate from the granules themselves, samples were spun down on a benchtop centrifuge at 5200g for 10 min. Under such conditions, the overwhelming majority of the granules were sedimented into a pellet (Figure 2a).

After centrifugation, an NMR spectrum was acquired on the separated supernatant and no signals in the region 3−6 ppm were observed. The spectrum of the resuspended pellet was essentially identical to the spectrum of the original sample. As slowly tumbling residues in the core of a starch granule would be invisible to solution-state NMR, such a finding allows us to conclude firmly that the observed saccharide resonances originate from flexible chains that are tethered on exposed surfaces of the starch granules; that is, the NMR resonances did not originate from free polysaccharide that had leached from the granules.

To characterize further the nature of the species to which the flexible chains are attached, NMR diffusion experiments were performed. Such experiments enable the determination of the extent of motion that individual chemical species undergo during a defined delay (i.e., Δ) in the experiment. The motion is conventionally related to the translational diffusion coefficient and corresponding hydrodynamic radii R_H of the species giving rise to the resonances.[26] In this case, the measured NMR diffusion coefficient will be independent of Δ. Such a situation was found for the NMR signals in the region 3−4.5 ppm originating from free maltose (Figure 2b, red), corresponding to a molecule with an R_H of 0.28 nm (Figure 2c, red). The measured diffusion coefficients of the starch granule

DOI: 10.1021/acs.biomac.5b00190
Biomacromolecules 2015, 16, 1614−1621

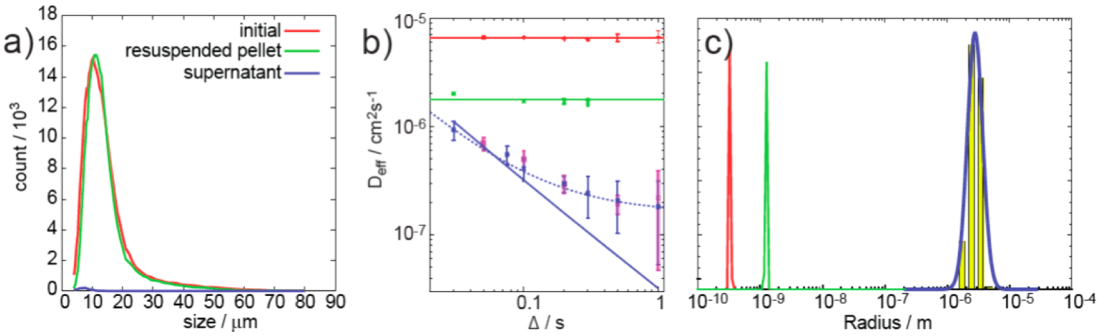

Figure 2. Size of the granules. (a) Coulter counter particle size histograms for a 10 mg/mL waxy rice starch suspension (red) of the supernatant after centrifugation at 5200*g* for 10 min (blue) and following resuspension (green). (b) The effective diffusion coefficients, D_{eff}, of the species giving rise to the saccharide resonances (3−4 ppm), as a function of the diffusion delay, Δ, as measured by solution-state NMR diffusion experiments, free maltose (red), starch granules digested by α-amylase (green), and native starch granules (blue) and granules hydrothermally treated at 70 °C (purple) before recording NMR spectra at 27 °C. A weighted least-squares line fitted to eq 1 yields the best fit, as shown by the blue solid line. The dotted blue line shows a fit to a more complex model (see main text). (c) Histogram showing calculated particle sizes estimated by optical microscopy (yellow) and NMR diffusion experiments (blue). The color identification of the red and green peaks is as seen in b.

were found to be smaller by about 2 orders of magnitude than those obtained for maltose (Figure 2b, blue), consistent with the signals originating from a species with a much larger hydrodynamic radius (Figure 2c). The observed diffusion coefficient was observed to vary strongly with Δ, however, indicating that the underlying species is undergoing significant additional motion during the measurement,[27] and so, we could not interpret the data in terms of the simple theory. The conclusion that the signals reflect a much larger particle accords well with the estimate of approximately 6 μm for the diameter of waxy rice granules derived from electron micrographs (Figure 1a).

An alternative model to explain the variance in observed diffusion coefficient D_{eff} with Δ considers the effects of other forms of local motion that occur in addition to that arising from translational diffusion[27] including, for example, rotational diffusion. In this case, the rotational diffusion coefficient of the 6 μm diameter starch particles is expected to be relatively slow. If we attribute the additional motion to a combination of intrinsic, rapid motions of the flexible chains themselves tethered to the surface of the granule, we can model the variation of D_{eff} with Δ to estimate the overall size of the underlying granule. Under this assumption, a weighted least-squares fitting of the observed data to eq 1 (see Materials and Methods) yields a radial granule size of 3 ± 0.5 μm (Figure 2b, solid blue line; Figure 2c, blue), although the curve fits less well to the data points obtained with the longest diffusion times. By leaving the model for translational diffusion unspecified and allowing only the rotational diffusion term to have an explicit dependence on R_H, however, the fitted curve matches the later data points significantly more closely, yielding a radius of 2.6 ± 0.3 μm (Figure 2b, dotted blue line), a value within the uncertainty of the estimate obtained using combined translational and rotational diffusion. Remarkably, the estimate of granule size from the NMR diffusion measurements is in excellent agreement with the overall particle size that was measured by SEM and optical microscopy (Figure 2c, yellow histogram).

In addition to the saccharide resonances, NMR signals were observed in the starch sample between 0 and 3 ppm (Figure 1b(i)). The diffusion coefficients were found to be independent of Δ, corresponding to a species with an R_H of 0.47 ± 0.06 nm. This size is commensurate with a relatively small molecule that is not too dissimilar in size to that measured for free maltose. The range of chemical shifts suggests that these species are free lipids arising from endogenous lipids released from granules during the purification process. Neither NOE nor scalar coupling cross peaks were observed between these resonances and the saccharide resonances indicating that the lipids are neither bound nor associated with the starch granules. These signals were invariant during both amylolysis and gelatinization (see below) and were employed as internal standards when considering the relative intensities of the saccharide resonances.[48]

Digestion of the starch granules with α-amylase for 1 h resulted in a spectrum with the saccharide resonances both increased in intensity and decreased in line width by a factor of about 10 compared with the initial spectrum (Figure 1b(iii), green and blue, respectively). An NMR diffusion analysis (Figure 2c, green) shows that these resonances correspond to a species with a size some 3 orders of magnitude smaller than that before digestion (R_H = 1.2 ± 0.3 nm, that is, noticeably larger than that of maltose). If resonances originating from flexible regions on the surfaces of the starch granule had remained after digestion, they would have been readily apparent from the NMR diffusion data and so these findings suggest that α-amylase removes the flexible chains from the surfaces of the starch granule. The relationship between the flexible chains on exposed surfaces of the granule and the action of α-amylase was compared (Figure 3).

When heated in water above 60 °C, the granules swell and undergo gelatinization (Figure 3a); a video clip of this process can be found online (SI, Figure S2). Slight variations in the critical temperature between 60 and 70 °C probably emanate from small compositional and structural differences between individual granules. When investigated by NMR, an increase in the signal intensity of the saccharide resonances was observed with increasing temperature (Figure 3b), showing that resonances from the saccharides increased significantly with temperature, whereas no change was observed in the intensity of the assumed lipid resonances between 0 and 3 ppm. The NMR diffusion coefficients measured for a sample heated to 70 °C (Figure 2b, purple) prior to a return to 27 °C for spectra acquisition, varied with Δ, corresponding to a species of hydrodynamic radius, within experimental uncertainty, of the value obtained from native starch. The NMR diffusion data

DOI: 10.1021/acs.biomac.5b00190
Biomacromolecules 2015, 16, 1614−1621

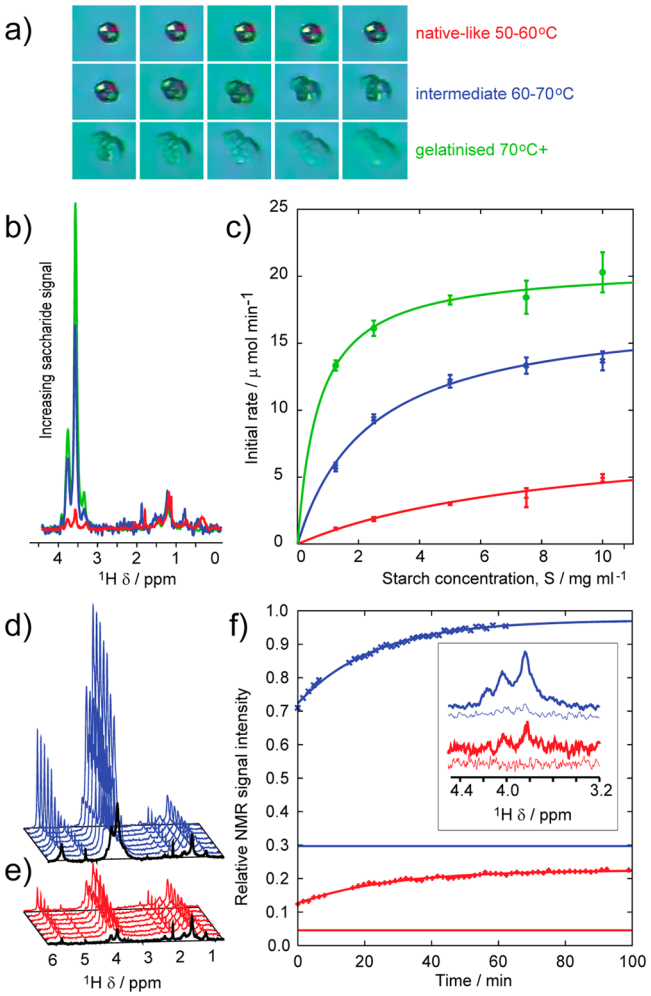

Figure 3. Effects of gelatinization on starch granules. (a) Cross polarized light microscopy images of single starch granule at intervals of 2 °C, 50−60 °C (red), 60−70 °C (blue), and 70−80 °C (green), showing loss of the Maltese cross pattern above 60 °C and swelling above 70 °C. (b) Solution-state NMR spectra of granules in the three temperature regimes. (c) The initial rate of maltose release measured at 37 °C in the presence of a fixed concentration of α-amylase as a function of the total concentration of starch (S) for native-like granules with no hydrothermal pretreatment (red), for granules in an intermediate structural state (pretreated at 65 °C, blue), and for gelatinized granules, pretreated at 80 °C (green). (d, e) Solution-state NMR spectra of starch granules in the presence of a fixed concentration of α-amylase. In (d), the granules have been pretreated at 70 °C, and in (e), the granules have experienced no hydrothermal treatment. (f) The increase in saccharide signal intensity during α-amylase hydrolysis as a function of time, for the preparations described in (d) and (e). Inset: PFGSE NMR spectra with Δ = 500 ms and a gradient strength of 15 G cm^{-1} taken before the addition of amylase and after 5 min of hydrolysis.

therefore show no evidence for significant populations of amylopectin or amylose free in solution that could have dissociated from the granule during the thermal treatment, a finding further confirmed by examination of supernatants after sedimentation of the gelatinized granules. The signal intensity gained during hydrothermal treatment can therefore be attributed to an increase in the number of flexible segments on exposed surfaces of the granules.

Granule samples were incubated at prespecified temperature before being digested with α-amylase at 37 °C and initial rates of reaction were determined from the increase of reducing sugars with time. The initial reaction rate increases hyperbolically as a function of starch concentration S in the sample (Figure 3c) and can be interpreted by Michaelis−Menten kinetics to yield values for k_{cat} and K_M^{exp} for each temperature at which the starch was pretreated (SI, Table S1).

The saccharide segments released from the starch granules during amylolysis were also detectable from the increase in the NMR signal. The initial rate of increase for a sample pretreated at 70 °C (Figure 3d,f) was about 4.4× greater than that measured for an untreated sample (Figure 3e,f), a result in agreement with that found from the assay for reducing units (Figure 3c). The time scale of the reaction was too rapid to allow the size of the individual species to be followed over the course of the reaction by NMR diffusion methods. After 10 min, however, it was possible to obtain a single PFGSE spectrum (see Materials and Methods) with a long diffusion delay (500 ms) and a high gradient strength (15 G cm^{-1}) and to compare this spectrum with one obtained before digestion. Under such conditions, a species whose R_H = 80 nm will have its signal reduced by a factor of about 100, and so only very large species will give rise to observable resonances. Although reasonably well resolved, NMR spectra were initially observed prior to digestion (Figure 3f, inset); after 10 min of digestion no resonances were observed, despite the signal intensity in the absence of the gradients having increased by a factor of 5−10 over the same period.

The correlation between α-amylase digestion data and the increase in NMR signal intensity with hydrothermal treatment was analyzed more quantitatively and the results are shown in Figure 4. In principle, α-amylase is capable of attacking any α-1−4 linkage in the granule but before hydrothermal treatment it appears that relatively few linkages are susceptible, indicating that structural constraints must be imposed by the semicrystalline nature of the granule. The fraction of accessible polyglucan residues (x) after a given pretreatment at temperature T is given by $x(T) = A/S$, where A is the concentration of accessible α-amylase substrate in a sample and S is the total starch concentration. This ratio is expected to be small for unprocessed starch but will increase as the granule is disordered by the gelatinization process. For each treatment temperature, the observed Michaelis value, K_M^{exp} (the concentration of starch that supports an initial reaction rate of $V_{max}/2$), will decrease if structural changes within the granule result in an increase in A. This quantity can be distinguished from K_M^{amy}, which is an "absolute" value that is the concentration of α-amylase substrate that supports half the maximum catalytic rate, a value that will be independent of structural changes that occur within the granule. Thus, the ratio of the two Michaelis constants reflects the fraction of the starch granule susceptible to hydrolysis at each pretreatment temperature $x(T) = K_M^{amy}/K_M^{exp}(T)$. We can then express the proportion of exposed polysaccharide sites at a given temperature, $x(T)$, relative to the number of exposed reaction sites in the untreated granule, $x(T_1)$, as the ratio $\gamma_1 = x(T)/x(T_1)$. Thus, the variation in γ_1 with pretreatment temperature indicates the change in exposed α-amylase reaction sites. Therefore,

$$\gamma_1 = \frac{K_M^{amy}(T_1)}{K_M^{exp}(T)} \quad (2)$$

Below 60 °C, very little change in γ_1 is observed (Figure 4a, black line). Above this temperature, however, γ_1 is found to

DOI: 10.1021/acs.biomac.5b00190
Biomacromolecules 2015, 16, 1614−1621

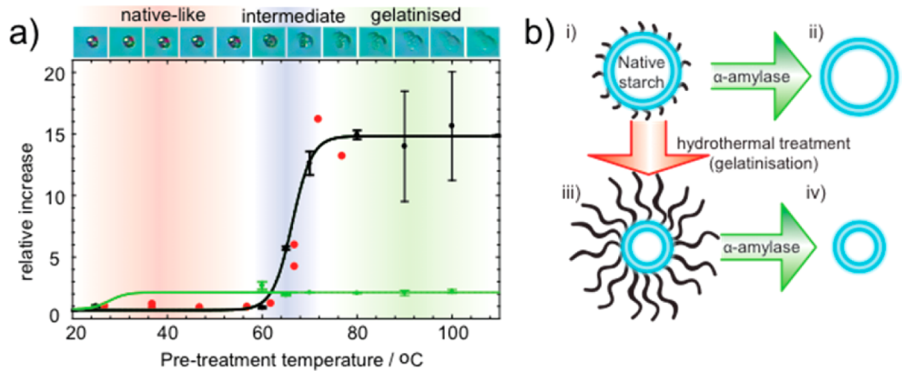

Figure 4. Exposed flexible chains. (a) The relative increase in flexible chains after hydrothermal treatment as measured by the change in apparent K_M^{exp} using γ_1 (black) and by the intensity of the solution state NMR signals of the saccharide protons as measured by γ_2 (red experimental points). The turnover number of α-amylase over the temperature range is shown by the green trace. The broad colored vertical bands reflect the three temperature regimes defined in Figure 3a. (b) A schematic diagram depicting the changes that occur in a waxy rice starch granule with gelatinization leading to an increase in exposed flexible chains and their hydrolysis by α-amylase.

increase by a factor of 14.7 ± 0.8, with a midpoint at 66 ± 0.5 °C. It is in this temperature range that starch granules are observed by optical microscopy to swell (Figure 3a) with intrinsic structural heterogeneities between individual starch granules leading to transition temperatures for individual particles in the range 60−72 °C. The K_M of bovine pancreatic α-amylase for solutions of purified amylopectin[45] is 0.73 mg mL^{-1}, enabling estimation of the average proportion of each granule susceptible to hydrolysis, $x(T)$ (Figure 4 and SI, Table S1). The data indicate that before pretreatment, only ∼6% of the granule is susceptible to amylolysis under these conditions, but after heat treatment the granule is found to behave almost like a solution of purified amylopectin with ∼95% of the granule being susceptible to hydrolysis.

The increase in NMR signal intensity of the saccharide resonances following hydrothermal treatment reflects an increase in the concentration of flexible saccharide chains that are surface exposed. This can be quantified through the definition of $\gamma_2 = S(T)/S(T_1)$, where $S(T)$ is the saccharide signal intensity at an arbitrary temperature, and $S(T_1)$ is the signal intensity from an untreated granule (Figure 4a, red). The increase of γ_2 with temperature occurs in a sigmoidal fashion and, remarkably, the two independent measurements of γ are in excellent quantitative agreement, with both found to increase by a factor of about 15 from below 60 °C to above 70 °C, where all starch granules are swollen and largely gelatinized.

The k_{cat} value varied little with the starch pretreatment temperature until the latter exceeded 25 °C (Figure 4a, green line; Table S1) and can be interpreted as a turnover number for α-amylase at the assay temperature of 37 °C. On heating a native starch granule, the granule visibly swells, the concentration of hydrated, flexible saccharide chains accessible to α-amylase (black) increases, and the semicrystalline core of the granule (blue) decreases (Figure 4). The early stage of amylolysis removes all accessible flexible saccharide units from exposed surfaces of the starch granule.

These experiments reveal a number of flexible α-glucan chains that project from the solvent-exposed starch granule surfaces and then have sufficient local mobility to yield well-defined NMR resonances, despite the slow underlying tumbling of the granules themselves. This observation supports the notion that waxy rice starch granules have certain features commensurate with an earlier description that flexible chains protrude from the underlying tightly packed core starch particle.[43] Gelatinization leads to an increase, by a factor of about 15, in the number of flexible chains (Figure 4), a process that occurs concurrently with disruption of the starch granules as determined through the loss of birefringence. As approximately 94% of the starch content of the granules is amylopectin, the increase in flexible chains accompanying gelatinization probably originates from an unravelling of semicrystalline, double helical amylopectin chains.[1,36,41] The action of the digestive enzyme α-amylase removes these protruding chains, and the gelatinization process leads to an increase of about 15 in the concentration of exposed α-amylase reaction sites (Figure 4a).

The close correlation between the NMR and enzyme kinetic measurements indicates that the flexible chains on the solvent-exposed surfaces of the starch granule are the primary substrate of α-amylase. Studies on the hydrolysis of oligosaccharides, together with X-ray crystallographic measurements, have revealed that the active sites of human and porcine α-amylases contain at least five subsites to which glucose residues of the oligosaccharide become bound during catalysis.[49,50] It is likely that a series of flexible residues can be more readily accommodated in the subsites of amylase, whereas more tightly packed residues in the core of the granule are significantly more restricted. We believe that our identification of flexible chains as the primary substrate of α-amylase elegantly reconciles much starch hydrolysis data with known mechanistic properties of the enzyme.[33]

The flexible chains are entirely removed by α-amylase within the first 10 min of hydrolysis under these conditions. The glucose concentration in the portal and peripheral blood circulation increases rapidly after starch consumption[9,51] on a comparable time scale. It is likely, therefore, at least in the case of waxy rice starch, that the relatively rapid increase in blood glucose following ingestion is a consequence of the removal and digestion of the flexible segments on the exposed surfaces of the granule. This finding has particular significance where a rapid and exaggerated increase in the postprandial blood glucose concentration is undesirable, such as in the glycemic control of people with diabetes.

Because the data were obtained using waxy rice starch only, it is useful to consider whether granules from other botanical sources and types would behave in similar ways. Our laboratory has collected enzyme kinetic data from a wide range of botanical starches that have included wheat, potato, maize,

DOI: 10.1021/acs.biomac.5b00190
Biomacromolecules 2015, 16, 1614−1621

normal rice and wild type, *lam* and *r* pea mutants, and where the amylopectin content has ranged from the 98% of waxy rice down to 28% for the pea *r* mutant.[33,34,42,52] In all cases, measured K_M values for hydrothermally treated starch are much smaller than the value found for native granules suggesting that the affinity for amylase is increased. It seems pertinent to the argument that we have shown a direct linear relationship between K_M values for starch hydrolysis and the dissociation constant (K_d) for starch binding to granules of various sizes and amylopectin content.[34] K_d is also related to the surface properties of granules.[33] It is not unreasonable therefore, to suppose that the change in kinetic and NMR signals that we observe for waxy rice starch are representative of a general granule property.

Using conventional NMR diffusion methodology, it is common to employ a single short delay, Δ, of about 50 ms in experiments. Under such conditions, the apparent diffusion coefficients for the hydrolyzed α-glucan chains in the digestion reaction and those from the starch granules are comparable (Figure 2b, green and blue, respectively). As the NMR experiment is sensitive to physical displacements, this finding is a consequence of the similarities in the relative motions on this time scale; the displacement of a flexible chain is comparable to the displacement of the hydrolysis products undergoing translational diffusion. As found with previous studies on amyloid fibrils,[28] only by considering the change in diffusion coefficient with diffusion delay can the true nature of the underlying dynamics be elucidated.

CONCLUSIONS

Our studies provide direct experimental evidence for the existence of flexible α-glucan chains protruding from solvent-exposed surfaces of starch granules and that these chains, which increase in number during hydrothermal processing, are the primary substrates of pancreatic α-amylase. We have further demonstrated the utility of recently developed solution state NMR methodology for studying large molecular assemblies.[28] Where large biomolecular assemblies have regions of sufficient local flexibility to yield narrow solution state NMR signals, the methodology of the type described in this work can be used to investigate structural properties that are currently inaccessible to other techniques. Our findings reveal that the flexible chains on the surface of starch granules ultimately dictate how rapidly their energy can be extracted by hominids.

ASSOCIATED CONTENT

Supporting Information

The information consists of an NMR spectrum for maltose showing proton resonances, a video showing granule swelling during hydrothermal treatment, plus a table listing Michaelis–Menten parameters for amylolysis at 37 °C of granules that had been hydrothermally treated at various temperatures. This material is available free of charge via the Internet at http://pubs.acs.org.

AUTHOR INFORMATION

Corresponding Authors

*E-mail: andrew.baldwin@chem.ox.ac.uk. Tel.: +44 (0)1865 275420.

*E-mail: peter.butterworth@kcl.ac.uk. Tel.: +44 (0)20 7848 4592.

*E-mail: peter.r.ellis@kcl.ac.uk. Tel.: +44 (0)20 7848 4238.

Present Address

‡The Physical and Theoretical Chemistry Laboratory, The University of Oxford, South Parks Road, Oxford, OX1 3QZ, United Kingdom.

Notes

The authors declare no competing financial interest.

ACKNOWLEDGMENTS

We thank Prof. Lewis Kay and Prof. Guy Lippens for stimulating discussions. A.J.B. thanks the BBSRC for a David Phillips Fellowship and Pembroke College. C.M.D. thanks the MRC, the Wellcome and Leverhulme Trusts, and the Cambridge Nanoscience Centre for support of this work. D.L.E. and F.J.W. thank the BBSRC and Unilever for receipt of an Industrial CASE award, and Kings College London for receipt of a KCL scholarship, respectively. We thank Dr. Phillippa Rayment (Unilever) for providing the waxy rice starch samples and the assistance of Dr. A. Brain in producing the SEM micrographs.

REFERENCES

(1) Oates, C. G. *Trends Food Sci. Technol.* **1997**, *8*, 375–382.

(2) Perry, G. H.; Dominy, N. J.; Claw, K. C.; Lee, A. A.; Fiegler, H.; Redon, R.; Werner, J.; Villanea; Mountain, J. L.; Misra, R.; Carter, N. P.; Lee, C.; Stone, A. C. *Nat. Genet.* **2007**, *39*, 1256–1260.

(3) Henry, A. G.; Brooks, A. S.; Riperno, D. R. *Proc. Natl. Acad. Sci. U.S.A.* **2011**, *108*, 486–491.

(4) Lucas, P. W. *Proc. Natl. Acad. Sci. U.S.A.* **2011**, *108*, 19101–19102.

(5) Carmody, R. N.; Wrangham, R. W. *J. Hum. Evol.* **2009**, *57*, 379–391.

(6) Laden, G.; Wrangham, R. W. *J. Hum. Evol.* **2005**, *49*, 482–498.

(7) Judd, P.; Ellis, P. R. In *Traditional Medicines for Modern Times. Antidiabetic Plants*; Soumyanath, A., Ed.; CRC Press, Taylor and Francis Group: Boca Raton, FL, U.S.A., 2006; pp 257–272.

(8) Seal, C. J.; Daly, M. E.; Thomas, L. C.; Bal, W.; Birkett, A. M.; Jeffcoat, R.; Mathers, J. C. *Br. J. Nutr.* **2003**, *90*, 853–864.

(9) Ells, L. J.; Seal, C. J.; Kettlitz, B.; Bal, W.; Mathers, J. C. *Br. J. Nutr.* **2005**, *94*, 948–955.

(10) Jenkins, D. J.; Kendall, C. W. C.; Augustin, L. S. A.; Franceschi, A. L.; Hamidi, M.; Marchie, A.; Jenkins, A. L.; Axelsen, M. *Am. J. Clin. Nutr.* **2002**, *76*, 266S–273S.

(11) Gallant, D. J.; Bouchet, B.; Buleon, A.; Perez, S. *Eur. J. Clin. Nutr.* **1992**, *46* (suppl. 2), S3–S16.

(12) Frost, G.; Leeds, A. A.; Dore, C. J.; Madeiros, S.; Dornhorst, A. *Lancet* **1999**, *353*, 1045–1048.

(13) Mann, J.; Cummings, J. H.; Englyst, H. N.; Key, T.; Liu, S.; Riccardi, G.; Summerbell, C.; Venn, B.; Vorster, H. H.; Wiseman, M. *Eur. J. Clin. Nutr.* **2007**, *61* (Suppl 1), S132–137.

(14) Salmeron, J.; Manson, J. E.; Stampfer, M. J.; Colditz, G. A.; Spiegelman, D.; Jenkins, D. J.; Wing, A. L.; Willett, W. C. *J. Am. Med. Assoc.* **1997**, *277*, 472–477.

(15) Carver, J. A.; Aquilina, J. A.; Truscott, R. J.; Ralston, G. B. *FEBS Lett.* **1992**, *311*, 143–149.

(16) Oswald, R. E.; Bogusky, M. J.; Bamberger, M.; Smith, R. A.; Dobson, C. M. *Nature* **1989**, *337*, 579–582.

(17) Radford, S. E.; Laue, E. D.; Perham, R. N.; Miles, J. S.; Guest, J. R. *Biochem. J.* **1987**, *247*, 641–649.

(18) Christodoulou, J.; Larsson, G.; Fucini, P.; Connell, S. R.; Pertinhez, T. A.; Hanson, C. L.; Redfield, C.; Nierhaus, K. H.; Robinson, C. V.; Schleucher, J.; Dobson, C. M. *Proc. Natl. Acad. Sci. U.S.A.* **2004**, *101*, 10949–10954.

(19) Sillen, A.; Leroy, A.; Wieruszeski, J. M.; Beauvillain, J. C.; Buee, L.; Landrieu, I.; Lippens, G. *ChemBioChem* **2005**, *6*, 1849–1856.

(20) Baldwin, A. J.; Bader, R.; Christodoulou, J.; MacPhee, C. E.; Dobson, C. M. *J. Am. Chem. Soc.* **2006**, *128*, 2162–2163.

DOI: 10.1021/acs.biomac.5b00190
Biomacromolecules 2015, 16, 1614–1621

(21) Meehan, S.; Knowles, T. P.; Baldwin, A. J.; Smith, J. F.; Squires, A. M.; Clements, P.; Treweek, T. M.; Ecroyd, H.; Tartaglia, G. G.; Vendruscolo, M.; MacPhee, C. E.; Dobson, C. M.; Carver, J. A. *J. Mol. Biol.* **2007**, *372*, 470−484.
(22) Baldwin, A. J.; Kay, L. E. *Nat. Chem. Biol.* **2009**, *5*, 808−814.
(23) Baldwin, A. J.; Walsh, P.; Hansen, D. F.; Hilton, G. R.; Benesch, J. L.; Sharpe, S.; Kay, L. E. *J. Am. Chem. Soc.* **2012**, *134*, 15343−15359.
(24) Baldwin, A. J.; Hilton, J. R.; Lioe, H.; Bagneris, C.; Benesch, J. L. P.; Kay, L. E. *J. Mol. Biol.* **2011**, *413*, 310−320.
(25) Dehner, A.; Kessler, H. *ChemBioChem* **2005**, *6*, 1550−1565.
(26) Stejskal, E. O.; Tanner, J. E. *J. Chem. Phys.* **1965**, *42*, 288−292.
(27) Baldwin, A. J.; Christodoulou, J.; Barker, P. D.; Dobson, C. M.; Lippens, G. *J. Chem. Phys.* **2007**, *127*, 11405.
(28) Baldwin, A. J.; Anthony-Cahill, S.; Christodoulou, J.; Lippens, G.; Barker, P. D.; Dobson, C. M. *Angew. Chem., Int. Ed.* **2008**, *47*, 3385−3387.
(29) Guilbot, A.; Mercier, M. In *The Polysaccharides*; Aspinall, G. O., Ed.; Academic Press, Inc.: Orlando, FL, 1985; Vol 3, pp 209−282.
(30) Blanshard, J. M. V. In *Starch Properties and Potential*; Galliard, T., Ed.; John Wiley & Sons Ltd.: New York, 1987; pp 16−54.
(31) French, D. In *Starch: Chemistry and Technology*; BeMiller, J. N., Whistler, R. L., Paschall, E. F., Eds.; Academic Press: San Diego, CA, 1984; pp 257−272.
(32) Manners, D. J. *Carbohydr. Polym.* **1989**, *11*, 87−112.
(33) Warren, F. J.; Butterworth, P. J.; Ellis, P. R. *Biochim. Biophys. Acta* **2013**, *1830*, 3095−3101.
(34) Warren, F. J.; Royall, P. G.; Gaisford, S.; Butterworth, P. J.; Ellis, P. R. *Carbohydr. Polym.* **2011**, *86*, 1038−1047.
(35) Dhital, S.; Warren, F. J.; Zang, B.; Gidley, M. J. *Carbohydr. Polym.* **2014**, *113*, 97−107.
(36) Lynn, A.; Stark, J. R. *Carbohydr. Res.* **1992**, *227*, 379−383.
(37) Biliaderis, C. G.; Page, C. M.; Maurice, T. J.; Juliano, B. O. *J. Agric. Food Chem.* **1986**, *34*, 6−14.
(38) Cooke, D.; Gidley, M. J. *Carbohydr. Res.* **1992**, *227*, 103−112.
(39) Donovan, J. W. *Biopolymers* **1979**, *18*, 263−275.
(40) Gidley, M. J. In *Gums and Stabilisers for the Food Industry*; Phillips, G. O., Williams, P. A., Wedlock, G. J., Eds.; IRL Press: Oxford, U.K., 1992; pp 87−92.
(41) Bogracheva, T. Y.; Meares, C.; Hedley, C. L. *Carbohydr. Polym.* **2006**, *63*, 323−330.
(42) Slaughter, S. L.; Ellis, P. R.; Butterworth, P. J. *Biochim. Biophys. Acta* **2001**, *1525*, 29−36.
(43) Lineback, D. R. *Baker's Dig.* **1984**, *58*, 16−21.
(44) Wang, Q.; Ellis, P. R.; Ross-Murphy, S. B.; Reid, J. S. G. *Carbohydr. Res.* **1995**, 229−239.
(45) Walker, J. A.; Harmon, D. L. *J. Anim. Sci.* **1996**, *74*, 658−662.
(46) Wider, G.; Dreier, L. *J. Am. Chem. Soc.* **2006**, *128*, 2571−2576.
(47) Wilkins, D.; Grimshaw, S.; Receveur, V.; Dobson, C. M.; Jones, J.; Smith, L. J. *Biochemistry* **1999**, *38*, 16424−16431.
(48) Amato, M. E.; Ansanelli, G.; Fisichella, S.; Lamanna, R.; Scarlata, G.; Sobolev, A. P.; Segre, A. *J. Agric. Food Chem.* **2004**, *52*, 823−831.
(49) Brayer, G. D.; Sidhu, G.; Maurus, R.; Rydberg, E. H.; Braun, C.; Wang, Y.; Nguyen, N. T.; Overall, C. M.; Withers, S. G. *Biochemistry* **2000**, *39*, 4778−4791.
(50) Gilles, C.; Astier, J. P.; Marchis-Mouren, G.; Cambillau, C.; Payan, F. *Eur. J. Biochem.* **1996**, *238*, 561−569.
(51) Ellis, P. R.; Roberts, F. G.; Low, A. G.; Morgan, L. M. *Br. J. Nutr.* **1995**, *74*, 539−556.
(52) Tahir, R.; Ellis, P. R.; Bogracheva, T. Y.; Meares-Taylor, C.; Butterworth, P. J. *Biomacromolecules* **2011**, *12*, 123−133.

DOI: 10.1021/acs.biomac.5b00190
Biomacromolecules 2015, 16, 1614−1621